Available online at www.sciencedirect.com
ScienceDirect
Thermochimica Acta 453 (2007) 120–127
thermochimica acta
www.elsevier.com/locate/tca

Model-free kinetics analysis of ZSM-5 catalyzed pyrolysis of waste LDPE

B. Saha, A.K. Ghoshal *

Department of Chemical Engineering, Indian Institute of Technology Guwahati, Guwahati-39, Assam, India

Received 15 October 2006; received in revised form 5 November 2006; accepted 17 November 2006
Available online 24 November 2006

Abstract

Both thermal and catalytic decomposition of waste LDPE sample is studied to understand the effect of catalyst (ZSM-5) on the decomposition behaviour. The nonlinear Vyazovkin model-free technique is applied to evaluate the quantitative information on variation of E_α with α for waste LDPE sample under both catalytic and noncatalytic nonisothermal conditions. The literature reported data on such variation under noncatalytic condition and effects of different catalysts on the LDPE sample are compared with the results of the present study.

Results show that the optimum catalyst composition is around 20 wt.%, where the reduction in maximum decomposition temperature is around 70 °C. Presence of ZSM-5 shows similar reduction in maximum decomposition temperature as reported for Al-MCM-41 and MCM-41. Similar trend to literature reported data is observed for variation of E_α with α for LDPE under nonisothermal noncatalytic condition. ZSM-5 catalyzed decomposition of the LDPE sample in the present study indicates that E_α is strong and increasing function of α and consists of four steps. Cracking of large polymer fragments on the external surface of the catalyst, oligomerization, cyclization, and hydrogen transfer reactions inside the catalyst pores might be the possible reaction mechanisms involved during catalytic decomposition.

Keywords: Activation energy; Catalytic decomposition kinetics; Waste LDPE; ZSM-5; Nonisothermal

1. Introduction

Thermal and/or catalytic pyrolysis of waste plastics is drawing more and more interest on the perspective of solid waste management since they are an alternative source of energy or chemical raw materials. In general, thermal pyrolysis is a high temperature process but catalytic degradation reduces the process temperature, is selective towards certain desired range of hydrocarbons, and improves the quality of products. Literature reports discussed below indicate that different researchers have used different catalysts to produce oil containing some valuable aromatic compounds (limonene, indene, styrene, xylene and naphthalene) that can be used in petrochemical industry [1–5], high calorific value gaseous product and a residual solid carbon being upgraded to produce a high-grade activated carbon [5,6]. Thus, the major focus in these studies was to find the pyrolysis product distribution. A few available literatures suggest suitable kinetic mechanism describing the process of decomposition for different catalyst–polymer systems.

Catalytic cracking of waste plastics over Ni-REY catalyst yielded liquid products, gas and residual wax of about 74, 22 and 4 wt.%, respectively [7]. Decomposition of polymer mixture over HZSM5 and PZSM5 zeolite catalyst showed increased amount of gaseous product [8] and the global reaction temperature was reduced from 600–700 °C to 420–450 °C. Waste samples of PE and PS being cracked thermally or in the presence of the cracking catalyst (platinum catalysts) and hydrogen in closed autoclaves, produced more than 90% yield of gas and liquid fraction in gasoline and diesel range boiling hydrocarbon [9,10]. Karishma and George [11,12] reported that zeolite based catalysts (US-Y and ZSM-5) led to severe over cracking resulting in increase in gaseous fraction because of the strong zeolite acidity. The catalysts (5A, 13X catalyst, Y-zeolites, and metallic catalysts like $ZnCl_2$ Fe_2O_3) had no influence on the conversion, product yield, or composition [13]. Degradation of HDPE with silicoaluminophoshate catalysts (SAPO-37) showed good catalytic activity with decrease in the activation energy and

* Corresponding author. Tel.: +91 361 2582251; fax: +91 361 2582291/2690762.
E-mail addresses: aloke@iitg.ernet.in, akg_66@yahoo.com (A.K. Ghoshal).

0040-6031/$ – see front matter © 2006 Elsevier B.V. All rights reserved.
doi:10.1016/j.tca.2006.11.012

production of mainly lighter products (C_2–C_{12}) [14]. Catalytic degradation of different PE (like LLDPE, LDPE, and HDPE) and PP using catalyst MCM-41 [15,16] showed a remarkable effect of the catalyst in accelerating the degradation process. Catalytic decomposition of PP over E-cat and ZSM-5 showed a remarkable decrease in the temperature of maximum decomposition rate, showing no saturating effect in the studied range [17].

Commercially available FCC catalyzed decomposition of LDPE produced the liquid products in gasoline hydrocarbons ranges with rich in aromatic and highly olefinic C_3–C_4 gases and coke residue [18]. Mesoporus catalysts (Al-MCM-41, and Al-SBA-16) that had shown high activity in catalytic cracking of virgin LDPE were practically inactive with waste plastics [19]. During catalytic degradation over different samples of zeolite beta, LDPE and PP showed higher conversions than HDPE. Degradation of HDPE showed high selectivity to C_5–C_{12} products (70%) but that of LDPE and PP produced higher proportions of lighter products C_1–C_4 [20]. Degradation of LDPE at 700 °C over micrometer HZSM-5 and nanocrystalline *n*-HZSM-5 generated a similar range of degradation products with a marked increase in the light olefins and aromatic fractions and complete elimination of heavier olefin and paraffin hydrocarbons but mesostructured catalysts, Al-MCM-41 generated low proportion of aromatics and a higher content of olefin and paraffin species [21]. Marcilla et al. [22] concentrated on the thermal and catalytic decomposition products of LDPE and HDPE. The catalysts used were HZSM5 and HUSY. They reported the reduction in the average molecular weight of the gases evolved during the catalytic process and higher amounts of alkenes and aromatic compounds were detected with HZSM5 than with HUSY. Zhou et al. [23] studied the decomposition of LDPE and PP over modified ZSM-5 and DeLaZSM-5 and showed that LDPE exhibited much higher catalytic degradation than PP. Zhou et al. [24] in another paper reported that catalytic activity of DeLaZSM-5 for LDPE decomposition is enhanced due to increase in weak acid sites and decrease in strong acid sites. Takuma et al. [25] reported that H-gallosilicate catalyzed decomposition of PE produces more liquid fractions including BTX, whereas, HZSM-5 catalyzed one produced less aromatics and more gas.

The pyrolysis kinetics study is important to know the decomposition mechanism, rate of reaction, reaction parameters and to predict the products distribution. This intern helps in proper selection of reactor, optimization of the reactor design and operating conditions [5,26–33]. Karishma and George [12] determined apparent activation energy for the overall polymer (LLDPE and PP) catalytic cracking process over zeolites, commercial cracking catalysts, clays and pillared clays using Ozawa method. The results showed that the activation energy increased with decrease in acidity of the catalysts. Marcilla et al. [16,17] investigated the kinetics of the thermal and catalytic decomposition of PP over MCM-41, ZSM-5, and FCC catalysts. In another work, they investigated the kinetics of the thermal and catalytic decomposition of PE over MCM-41 catalysts [15]. They applied quantitative mechanistic kinetics model and evaluated the kinetics constants, which revealed a reduction in the activation energy of the catalytic decomposition as compared to the thermal process. The thermal and catalytic decomposition kinetics studies of HDPE over SAPO-37 and PP over ZSM-5 and ZSM-12 catalysts applying Vyazovkin model-free approach through use of isoconversion method [14,33] showed variation of activation energy (E_α) with conversion (α) and reduction in decomposition temperature and activation energy. However, to the best of our knowledge no such literatures have reported variation of E_α with α during catalytic decomposition of LDPE using model-free technique.

Model free analysis technique is advantageous over model fitting analysis when the real kinetics mechanism is unknown. This becomes extremely important during catalytic decomposition since reaction mechanism may change drastically with type and concentration of catalyst. Thus, for such complex reaction processes, applying Vyazovkin model-free kinetic method, accurate evaluations of complex reactions can be performed, as a way of obtaining reliable and consistent kinetic information about the overall process [20–31,33–40]. Apart from this, isoconversion method presents a compromise between the single-step Arrhenius kinetic treatments and the prevalent occurrence of processes whose kinetics are multi-step or non-Arrhenius [40].

In the present investigation, we studied both thermal and catalytic decomposition of waste LDPE sample. We examined the optimum catalyst (ZSM-5) concentration. Then we applied the nonlinear Vyazovkin model-free technique to study the nonisothermal catalytic and noncatalytic decomposition of waste LDPE sample. We have also shown, probably the first time, the quantitative information on variation of E_α with α for LDPE sample under both catalytic and noncatalytic nonisothermal conditions. The literature reported data on such variation under noncatalytic condition are compared with the present result.

2. Materials and experimental

2.1. Materials

The nonisothermal decomposition with and without catalyst was carried out with waste LDPE sample. The catalyst used was ZSM-5 supplied by Ranbaxy Laboratories Ltd., India.

2.2. Characterization of ZSM-5 zeolite sample

ZSM-5 zeolite sample was characterized by X-ray diffraction (XRD) analysis, scanning electron microscope (SEM) micrograph (make: LEO; model: 1430VP) and nitrogen adsorption study at 77 K. The XRD was carried out on Bruker AXS instrument using Cu Kα radiation (40kV, 40 mA) with step size of 0.05° (2θ) and time of 0.5 s per step.

Nitrogen adsorption isotherm at 77 K was determined on SA 3100 surface analyzer from Beckman Coulter using helium (for dead space calibration) and nitrogen. The ZSM-5 sample was out gassed for two hours at 250 °C.

2.3. Characterization of waste LDPE sample

Differential scanning calorimetry (DSC) analysis of the LDPE sample was performed under stagnant air atmosphere,

using instrument DSC 821^e of Mettler TOLEDO, to measure the melting point and percentage crystallinity.

2.4. Experimental procedure and equipment

Thermal and catalytic decomposition experiments were carried out in a TGA instrument of Mettler TOLEDO with model no TGA/SDTA 851^e under nitrogen atmosphere for a range of temperature 303–873 K. Nitrogen flow rate was maintained at 40–50 ml min^{-1} according to the specification of the equipment. LDPE samples were shredded into very small pieces and directly fed to the TGA instrument. Platinum crucible (150 μl) was used as sample holder. Total mass of sample taken was 7–10 mg for each run of the experiments. Thermal decomposition experiments were conducted in dynamic condition at different heating rates of 5, 10, 15, 20 and 25 K min^{-1}. Catalytic decomposition experiments were carried out with different percentage of catalyst (5–50 wt.%) at 10 K min^{-1}. The optimum catalyst percentage was found around 20 wt.% catalyst after which reduction in temperature with increase in catalyst percentage was not so significant. Therefore, further catalytic decomposition experiments were conducted using 20 wt.% catalyst at different heating rates of 5, 10, 15, 20, and 25 K min^{-1}. The TGA experiments were repeated thrice at 10 °C heating rate. The deviations observed are very little. However, the deviations are reported in terms of average relative deviation, ARD (%) $= (100/N)\sum_{i=1}^{N}(x_i^{\exp} - x_{\mathrm{av},i})/x_{\mathrm{av},i}$, where $x_i^{\exp}$ and $x_{\mathrm{av},i}$ are the experimental values of the variables (temperature and normalized mass) and average values of the variables, respectively, i = no. of data points for each experiment. Results show that ARD% are 0.051–0.119 (for temperature), 0.865–2.457 (for mass).

3. Kinetics analysis

3.1. Kinetics models and model-free kinetics analysis

The kinetics model equation combined with the Arrhenius approach of the temperature function of reaction rate constant is expressed as

$$\frac{\mathrm{d}\alpha}{\mathrm{d}t} = k_0 \exp\left(\frac{-E_\alpha}{RT}\right) f(\alpha) \tag{1}$$

where t is the time (min), T the temperature (K), α the conversion of reaction $(W_0 - W)/(W_0 - W_\infty)$, W_0 the initial weight of the sample (mg), W the sample weight (mg) at any temperature T, W_∞ the final sample weight (mg), $\mathrm{d}\alpha/\mathrm{d}t$ the rate of reaction (min^{-1}), $f(\alpha)$ the reaction model, k_0 is the pre-exponential factor (K^{-1}) and E_α is the activation energy (kJ mol^{-1}) are the Arrhenius parameters. R is the gas constant (kJ mol^{-1} K^{-1}). The reaction model may take various forms based on nucleation and nucleus growth, phase boundary reaction, diffusion, and chemical reaction [35–39]. However, the present investigation does not require any information of reaction model since we report here decomposition kinetics using model-free approach.

At a constant heating rate under nonisothermal conditions the explicit temporal/time dependence in Eq. (1) is eliminated through the trivial transformation:

$$\beta\frac{\mathrm{d}\alpha}{\mathrm{d}T} = k_0 \exp\left(\frac{-E_\alpha}{RT}\right) f(\alpha) \tag{2}$$

where $\beta = \mathrm{d}T/\mathrm{d}t$ is the heating rate (K min^{-1}) and $\mathrm{d}\alpha/\mathrm{d}T$ is the rate of reaction (K^{-1}).

3.1.1. Model-free isoconversion method for nonisothermal experiments [30,31,35–38]

For a set of five experiments carried out at five different heating rates (5, 10, 15, 20 and 25 K min^{-1}) the E_α can be determined at any particular value of α by finding the value of E_α for which the objective function Ω is minimized [38], where

$$\Omega = \sum_{i=1}^{n}\sum_{j=1,\, j\neq 1}^{n}\frac{I(E_\alpha, T_{\alpha i})\beta_j}{I(E_\alpha, T_{\alpha j})\beta_i} \tag{3}$$

and

$$I(E_\alpha, T_{\alpha i}) = \int_0^{T_{\alpha i}} \exp\frac{-E_\alpha}{RT}\mathrm{d}T \tag{4}$$

The temperature integral can be evaluated by several popular approximations and direct numerical integration. We used the later technique for the same, where the temperature integral takes the form:

$$I(E_\alpha, T_{\alpha i}) = \int_0^{T_{\alpha i}} \exp\frac{-E_\alpha}{RT}\mathrm{d}T = \frac{E_\alpha}{R}\left[\frac{\exp(-u)}{u} - E_i(u)\right] \tag{5}$$

where

$$u = \frac{E_\alpha}{RT} \quad \text{and} \quad E_i(u) = \int_u^\infty \frac{\exp(-u)}{u}\,\mathrm{d}u$$

Details of development of Eq. (5), numerical procedure and algorithms for model-free technique are discussed in our recent publication [31].

4. Results and discussion

4.1. Characterization of ZSM-5 zeolite catalyst and LDPE sample

The XRD pattern (Fig. 1) shows that the catalyst was crystalline without any evidence of another phase. The morphology of the catalyst is reported through Fig. 2 in the form of scanning

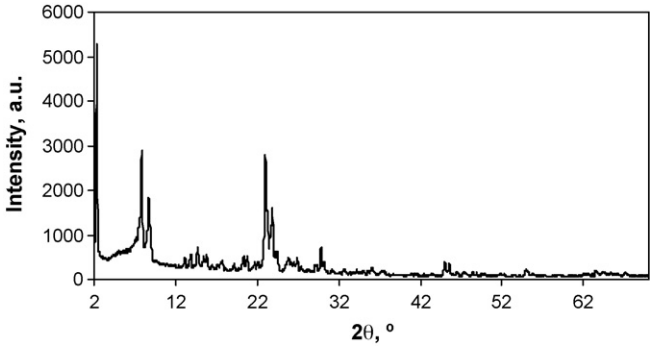

Fig. 1. XRD pattern of ZSM-5 zeolite catalyst.

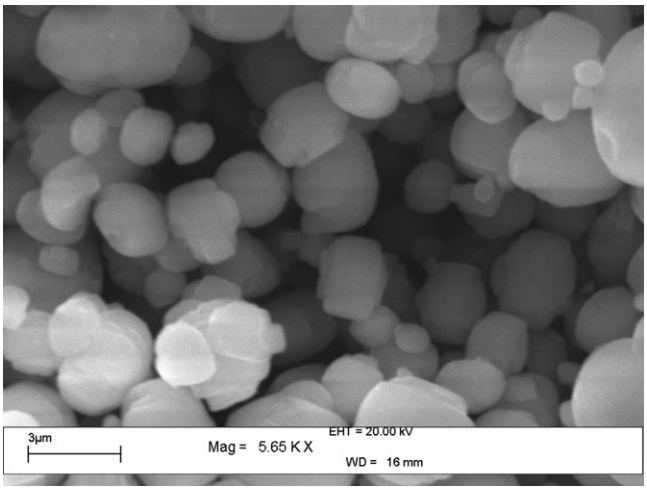

Fig. 2. SEM micrograph of ZSM-5 zelolite catalyst.

Table 1
Textural properties of ZSM-5

Sample	ZSM-5
BET surface area ($m^2\ g^{-1}$)	342.36
External surface area (by t-plot surface area) ($m^2\ g^{-1}$)	166.88
Micropore volume (by t-plot surface area) ($cm^3\ g^{-1}$)	0.084
Pore volume (at $P_s/P_o = 0.9814$, adsorption) ($cm^3\ g^{-1}$)	0.207

electron microscope (SEM) micrograph. Table 1 summarizes the surface area and pore volume of ZSM-5 sample used. The textural properties (Table 1) of ZSM-5 shows lower external surface area due to micrometer crystal sizes present in sample, which is also evident from SEM picture (Fig. 2). Fig. 3 shows the nitrogen isotherm of ZSM-5 sample. The pore size distribution calculated using Barrett, Joyner and Halenda (BJH) method (Fig. 4) only indicates the presence of the mesopores in ZSM-5 not the micropores, which should be more in ZSM-5 zeolite catalyst. The isotherm (Fig. 3) is Brunauer Type I with wide range of pore sizes, which is also supported by the BJH pore size distribution (Fig. 4). The nature of the isotherm indicates a continuous progression with increasing loading from monolayer to multilayer adsorption and then to capillary condensation. Fig. 5 shows the DSC analysis of waste LDPE sample indicating its melting point. The melting point, percentage crystallinity, and

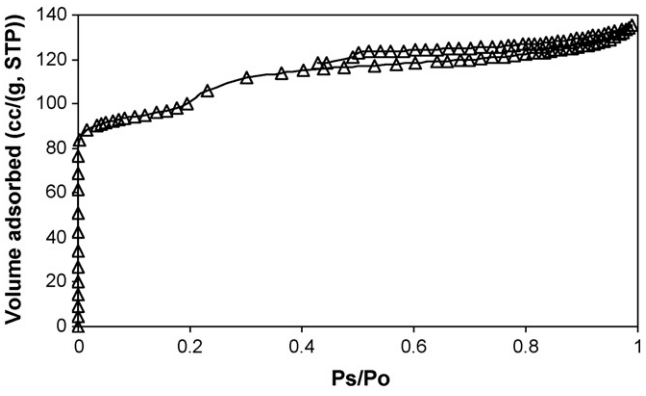

Fig. 3. Nitrogen adsorption isotherm at 77 K of ZSM-5 catalyst.

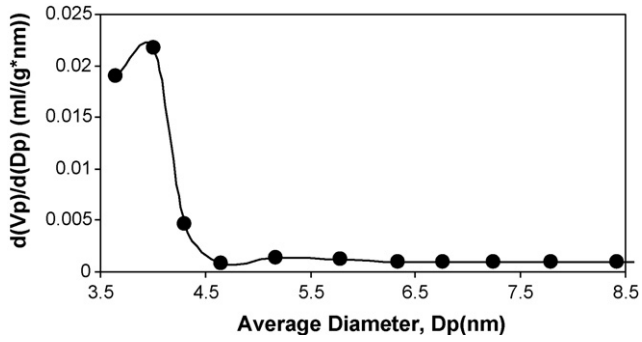

Fig. 4. BJH (desorption) pore size distribution of ZSM-5 catalyst.

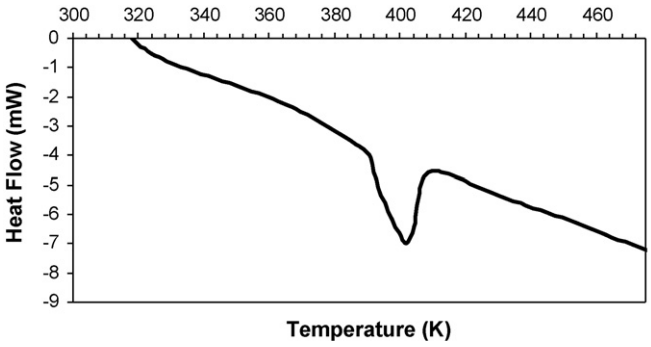

Fig. 5. DSC analysis of waste LDPE sample.

purity (in terms of residue) of the sample are summarized in Table 2.

4.2. Determination of optimum catalyst concentration

The temperature at which the conversion (α) is zero (T_{w0}), decomposition starts (T_d), maximum weight loss rate occurs (T_m) and the end of pyrolysis step ($T_{w\infty}$) takes place is reported in the Table 3 for each case of the experiments. Table 3 reflects that thermal decomposition of waste LDPE starts at around 640 K and showed a maximum decomposition rate at $T_m = 748$ K at a heating rate of 10 K min^{-1}, which are shifted to much lower temperatures in the presence of catalyst. The maximum shift is observed to be 91 K at a catalyst percentage of 50 wt.%.

Figs. 6 and 7 illustrate the thermogravimetric (TG) and the derivative thermogravimetric (DTG) plots for the catalytic degradation of waste LDPE. It also observed from Fig. 7 that the shape of the derivative thermogravimetric (DTG) curves changes significantly due to different wt.% of ZSM-5 catalyst during the

Table 2
Characteristics of waste LDPE sample

Sample type	Waste LDPE
Melting point	128.7 °C
Melting point of standard PE samples [20]	LDPE: 98–120 °C
Heat of fusion ($J\ g^{-1}$)	38.37
Heat of fusion, 100% crystals ($J\ g^{-1}$)	290
Degree of crystallinity	23.95%
Crystallinity of standard PE samples [20]	LDPE: 50–70%
Purity (residual amount after TGA experiment up to 600 °C)	Nonisothermal: 1–2%

Table 3
Experimental conditions for TGA studies

Sample	Nonisothermal experiments				
	Initial mass (mg)	Heating rate (K min^{-1})	Temperature range (K)	Residue (%)	$T_{w0}/T_d/T_m/T_{w\infty}$ (K)
Waste LDPE + ZSM-5 (20 wt.%)	5.57	5	303–873	25.17	470.4/575.4/659.9/777.9
	7.55	10	303–873	21.04	462.7/586.9/678.4/769.9
	9.64	15	303–873	23.37	462.2/590.6/679.9/769.9
	7.83	20	303–873	20.35	471.1/599.1/686/779.7
	7.51	25	303–873	20.92	462.2/604.1/693.9/779.5
Waste LDPE	7.77	5	303–873	1.73	551.1/633/734.24/811.2
	8.45	10	303–873	1.64	551.3/640.2/748.4/809
	11.19	15	303–873	2.13	549/654/754.04/808.8
	8.68	20	303–873	2.14	549.4/665/763.2/808.4
	10.91	25	303–873	1.19	576.5/686.1/770.4/815.4

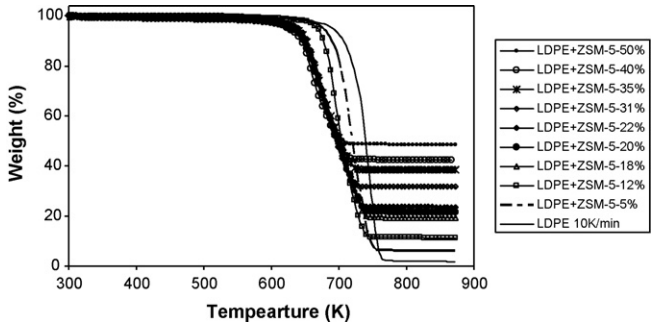

Fig. 6. Experimental TG curves for the catalytic pyrolysis of waste LDPE with different catalyst (ZSM-5) percentage.

catalytic decomposition of waste LDPE sample. This change is very prominent at lower catalyst compositions. From catalyst composition of 18 wt.% onwards, the curves are overlapping in nature though there are different peaks at different temperatures for different compositions. This behaviour indicates possibility of existence of different decomposition mechanism for different catalyst wt.%. Therefore, meaningful correlation of these TGA data with different wt.% of catalyst and without catalyst by a simple kinetics model using model-fitting techniques alone may be unreliable and unrealistic.

Since, the catalysts are expensive and, at the moment, there are no useful ways to improve their short life or to make effective recycling [16,17], therefore, we concentrated on getting the optimum catalysts percentage. Economically, optimum catalyst percentage should be decided based on the extent of decrease of decomposition temperature with catalyst percentage. Fig. 8 shows the effect of catalyst percentage on the maximum decomposition temperature, T_m of the waste LDPE sample. It is observed that the temperature decreases exponentially with catalyst percentage. It is further observed that the optimum catalyst percentage could be around 20 wt.%, since, after that reduction in T_m with increase in catalyst percentage is not so significant. Hence using catalyst percentage more than this would not be economically effective. To illustrate quantitatively, it may be seen that for a change of catalyst percentage from 20 to 31 wt.%, the further reduction in T_m is about 5 °C, where as for a change of catalyst percentage from 12 to 20 wt.%, the further reduction in T_m is about 20 °C. Also, as discussed earlier, from the overlapping in nature of the DTG curves (Fig. 7) for catalyst composition of 18 wt.% onwards, identification of 20 wt.% catalyst may be a judicious selection. The reduction in maximum decomposition temperature is around 70 °C at 20 wt.% catalyst. Thus, we selected 20 wt.% as the optimum catalyst (ZSM-5) percentage for the present study.

The exponential decrease in T_m for the LDPE catalytic pyrolysis with ZSM-5 can be explained in the similar line of Marcilla et al. [15,16], assuming that the large molecules have to react on the external surface of the zeolite catalyst, which could be the limiting reaction step. When more zeolite is added, more surface is available and more polymer molecules participate in the initial reaction step, until a situation is reached with an

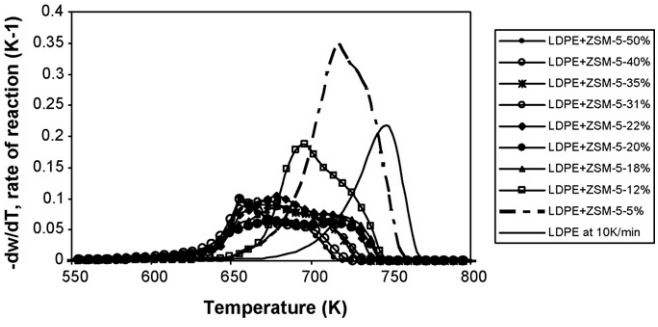

Fig. 7. Experimental DTG curves for the catalytic pyrolysis of waste LDPE with different catalyst (ZSM-5) percentage.

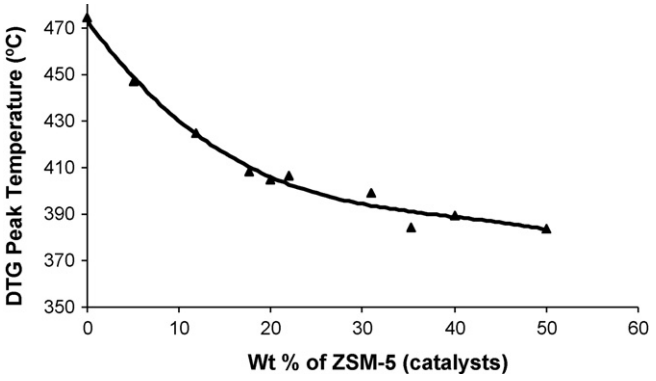

Fig. 8. Effect of catalyst (ZSM-5) on the maximum decomposition temperature.

Table 4
Effect of catalysts on PE decomposition temperatures

Sample	Catalysts	Weight percentage	T_d (°C)	T_m (°C)	Reference
HDPE	–	0	420	–	Araujo et al. [13]
	SAPO-37	25	375	–	
LLDPE(Escorene)	–	0	–	485.2	
	MCM-41	9.31	–	406.4	
LLDPE(Borecene)	–	0	–	484.3	
	MCM-41	9.18	–	419.6	
LLDPE(Dowlex)	–	0	–	483.7	Marcilla et al. [14]
	MCM-41	9.38	–	423.5	
HDPE	–	0	–	486.0	
	MCM-41	8.98	–	408.1	
LDPE	–	0	–	482.4	
	MCM-41	8.67	–	407.6	
LDPE	–	0	425	477	Serrano et al. [20]
	n-HZSM-5	–	–	396	
	HZSM-5	–	–	443	
	Al-MCM-41	–	–	407	
LDPE	–	0	367	475.2	Present work
	ZSM-5	20	313.7	405.2	

excess of zeolite, where there is not enough polymer to cover all the available zeolite active sites, thus not contributing this excess of zeolite to the initial reaction step of large macromolecules. Table 4 summarizes the literature available data on the catalytic effect on polyethylene (PE). Table 4 reflects that amongst the catalysts used for LDPE decomposition, Al-MCM-41 and MCM-41 shows similar reduction in temperature as we have observed with ZSM-5. But HZSM-5 performance is not at par with them, where the reduction in temperature is quite low. However, n-HZSM5 shows superior results in comparison to all.

4.3. Catalytic and noncatalytic nonisothermal decomposition at several heating rates

Nonisothermal decomposition of the waste sample was carried out at five different heating rates (5, 10, 15, 20, and 25 K min^{-1}) with the decided optimum catalyst percentage and without catalyst also. The nonisothermal noncatalytic pyrolysis yielded around 97–99% weight loss. The temperatures T_{w0}, T_d, T_m and $T_{w\infty}$ for the experiments are also reported in the Table 3. Variation of conversion, α with temperature for catalytic (20 wt.%) and noncatalytic decomposition at different heating rates are reported through Figs. 9 and 10, respectively. Variations of rate, dα/dT with temperature during nonisothermal pyrolysis using catalyst ZSM-5 (20 wt.%) at different heating rates are reported through Fig. 11. It is observed from the Figs. 7, 9 and 10 that catalytic decomposition starts and completes at much lower temperatures than that for noncatalytic decomposition. However, catalytic decomposition continues for a wider range of temperature than noncatalytic decomposition leading to flatter α versus temperature curves. The slow decomposition behaviour in presence of catalyst is also evident from Fig. 7, where the rate of decomposition in most of the cases is much lower than that

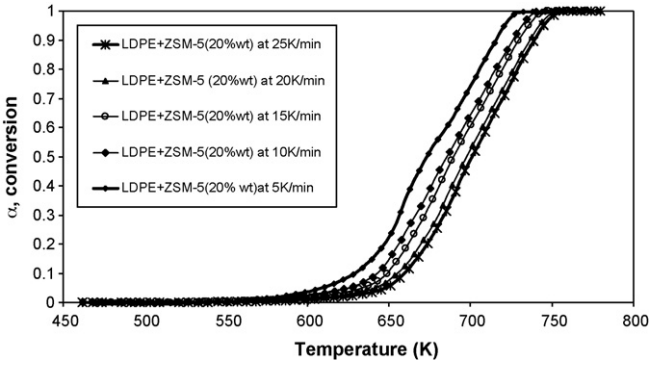

Fig. 9. Variation of conversion (α) with temperature during catalytic nonisothermal pyrolysis of waste LDPE sample.

in absence of catalyst. Polyethylene degradation on the ZSM-5 catalysts takes place due to presence of zeolite acidic sites.

Large polymer fragments are cracked on the external surface of the catalyst at the start of degradation forming smaller

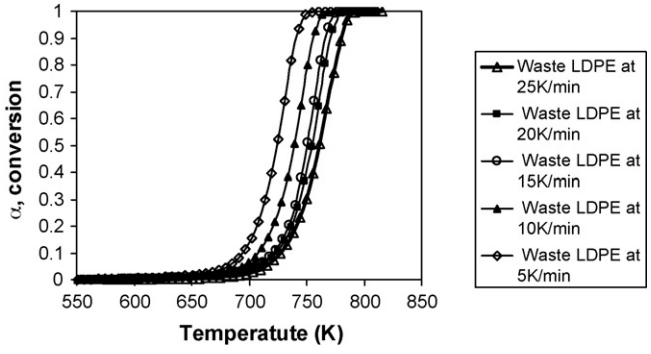

Fig. 10. Variation of conversion (α) with temperature during nonisothermal pyrolysis of waste LDPE pure sample.

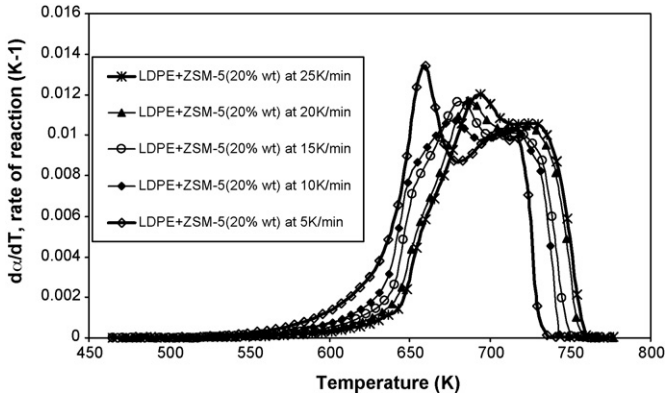

Fig. 11. Variation of rate of decomposition (dα/dT) with temperature during catalytic nonisothermal pyrolysis of waste LDPE sample.

molecules and radicals. These molecules in the subsequent stages enter into the pores and participate in other reactions like isomerization and oligomerization [33]. Therefore, catalytic (ZSM-5) degradation of LDPE results in formation of aromatics, light parafins and olefins due to the reactions like oligomerization, cyclization, and hydrogen transfer reactions [20]. But thermal decomposition of LDPE without catalyst occurs through random scission of original polymer chain into straight chain fragments of varying length generating radicals along the polymer backbone followed by scission of the molecule and hydrogen transfer resulting in formation of dienes, alkenes and alkanes [21,31,41]. The slowness of the catalytic decomposition over noncatalytic decomposition may be attributed to the different reaction mechanisms as discussed.

4.4. Kinetics for nonisothermal model-free analysis

Dependency of E_α on α obtained for nonisothermal decomposition of the waste LDPE sample with and without catalyst is presented through Fig. 12. It is observed from the figure that in case of noncatalytic decomposition, E_α is almost constant (around 190 kJ mol^{-1}) with α. Almost similar values and similar trend were also observed by Lyon et al. [42] during nonisothermal noncatalytic decomposition of LDPE (Fig. 12). The

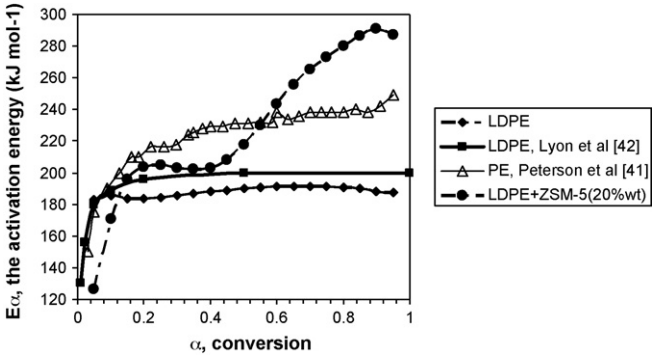

Fig. 12. Dependency of activation energy on conversion of catalytic and noncatalytic nonisothermal decomposition of waste LDPE sample (present work and literature reported data).

reported data of Peterson et al. [41] is also compared with the present result through the same figure. It is observed from the figure that the trend of variation of E_α with α is similar with a substantial difference in E_α values. The constant difference between the present E_α values and that reported by Peterson et al. [41] might be due to difference in molecular weight of the samples as well chain branching [31].

But in case of ZSM-5 catalyzed decomposition of the same sample, it is observed that E_α is strong and increasing function of α except the plateau region for $\alpha = 0.15$ till $\alpha = 0.4$. This may be explained as follows.

Large polymer fragments are cracked on the external surface of the catalyst at the start of decomposition forming smaller molecules and radicals. This is possibly a common phenomenon both for catalytic and noncatalytic process. Thus, only effect of catalyst is observed in the form of reduction of the temperature and the activation energy at this stage of decomposition. At the later stage of catalytic decomposition, the reaction mechanism possibly takes different path for oligomerization, cyclization, and hydrogen transfer reactions, which led to higher activation energy even in comparison to noncatalytic decomposition. The different reaction steps involved during catalytic decomposition is also obvious from the four steps observed in the variation of E_α with α (Fig. 12) during catalytic decomposition. Existence of wide range of pore sizes (Figs. 3 and 4) might also play important roles in the types of reactions taking place and the product distribution during catalytic decomposition of PE. The four-step process as evident from Fig. 12 goes in line with the reported discussion of Takuma et al. [25]. According to the scheme given by Takuma et al. [25], these steps in sequence is thermal degradation of PE (step 1), catalytic cracking of the high molecular weight fragments to give liquid and/or gas (steps 2 and 3), and finally formation of aromatics through cyclization (step 4). However, higher activation energy indicates slowness of the reaction rate, which is also indicated through decreasing peak height in the DTG curves (Fig. 7) and in the flatter TGA curves (Fig. 6) for catalytic decomposition of LDPE sample.

5. Conclusion

Both thermal and catalytic decomposition of waste LDPE sample is studied to understand the effect of catalyst (ZSM-5) on the decomposition behaviour. Results show that catalytic decomposition starts and completes at much lower temperatures than that for noncatalytic decomposition but continues for a wider range of temperature. It is observed that the temperature decreases exponentially with catalyst percentage. It is further observed that the optimum catalyst percentage was around 20 wt.%, where the reduction in maximum decomposition temperature is around 70 °C. From the comparison of the effects of other catalysts on LDPE samples, it is found that Al-MCM-41 and MCM-41 shows similar reduction in temperature as observed with ZSM-5. But HZSM-5 performance is not at par with them, where the reduction in temperature is quite low. However, *n*-HZSM5 shows superior results in comparison to all.

The nonlinear Vyazovkin model-free technique is applied to evaluate the quantitative information on variation of E_α

with α for LDPE sample under both catalytic and noncatalytic nonisothermal conditions. Variation of E_α with α for LDPE under nonisothermal noncatalytic condition is compared with the reported results by Lyon [42] and Peterson et al. [41]. Results show that almost similar values and similar trend were also observed by Lyon et al. [42] during nonisothermal noncatalytic decomposition of LDPE. The constant difference between the present E_α values and that reported by Peterson et al. [41] might be due to difference in molecular weight of the samples as well chain branching [30]. In case of ZSM-5 catalyzed decomposition of the LDPE sample, it is observed that E_α is strong and increasing function of α and consists of four steps. Cracking of large polymer fragments on the external surface of the catalyst, oligomerization, cyclization, and hydrogen transfer reactions inside the catalyst pores might be the possible reaction mechanisms involved during catalytic decomposition.

References

[1] C.M. Simon, W. Kaminsky, B. Schlesselmann, J. Anal. Appl. Pyrol. 38 (1996) 75.
[2] B.J. Milne, A.L. Behie, F. Berruti, J. Anal. Appl. Pyrol. 51 (1999) 157.
[3] P.T. Williams, E.A. Williams, J. Anal. Appl. Pyrol. 51 (1999) 107.
[4] W. Kaminsky, B. Schlesselmann, C.M. Simon, Polym. Degrad. Stab. 53 (1996) 189.
[5] B. Saha, A.K. Ghoshal, Chem. Eng. J. 111 (2005) 39.
[6] J.B. Parra, C.O. Ania, A. Arenillas, F. Rubiera, J.J. Pis, Appl. Surf. Sci. 252 (2005) 619.
[7] T. Masuda, T. Kushino, T. Matsuda, S.R. Mukai, K. Hashimoto, S. Yoshida, Chem. Eng. J. 82 (2001) 173.
[8] C. Vasile, H. Pakdel, B. Mihai, P. Onu, H. Darie, S. Ciocalten, J. Anal. Appl. Pyrol. 57 (2001) 287.
[9] J. Walendziewski, M. Steininger, Catal. Today 65 (2001) 323.
[10] J. Walendziewski, Fuel 81 (2002) 473.
[11] G. Karishma, M. George, Polym. Degrad. Stab. 83 (2004) 267.
[12] G. Karishma, M. George, Polym. Degrad. Stab. 86 (2004) 225.
[13] P. Filomena, C. Paula, I. Gulyurtlu, I. Cabrita, J. Anal. Appl. Pyrol. 51 (1994) 57.
[14] A.S. Araujo, V.J. Fernandes Jr., G.J.T. Fernandes, Thermochim. Acta 392/393 (2002) 55.
[15] A. Marcilla, A. Gomez, A.N. Garcia, M.M. Olaya, J. Anal. Appl. Pyrol. 64 (2002) 85.
[16] A. Marcilla, A. Gomez, J.A. Reyes-Labarta, A. Giner, Polym. Degrad. Stab. 80 (2003) 233.
[17] A. Marcilla, A. Gomez, J.A. Reyes-Labarta, A. Giner, F. Hernandez, J. Anal. Appl. Pyrol. 68/69 (2003) 467.
[18] J.S. Kim, W.Y. Lee, S.B. Lee, S.B. Kim, M.J. Choi, Catal. Today 87 (2003) 59.
[19] G.D.L. Puente, C. Klocker, U. Sedran, Appl. Catal. B 36 (2002) 279.
[20] J. Aguado, D.P. Serrano, J.M. Escola, E. garagorri, J.A. Fernandez, Polym. Degrad. Stab. 69 (2000) 11.
[21] D.P. Serrano, J. Aguado, J.M. Escola, J.M. Rodríguez, G.S. Miguel, J. Anal. Appl. Pyrol. 74 (2005) 370.
[22] A. Marcilla, M.I. Beltran, R. Navarro, J. Anal. Appl. Pyrol. 76 (2006) 222.
[23] Q. Zhou, L. Zheng, Y.Z. Wang, G.M. Zhao, B. Wang, Polym. Degrad. Stab. 84 (2004) 493.
[24] Q. Zhou, Y.Z. Wang, C. Tang, Y.H. Zhang, Polym. Degrad. Stab. 80 (2003) 23.
[25] K. Takuma, Y. Uemichi, A. Ayame, Appl. Catal. A 192 (2000) 273.
[26] J.R. Opfermann, E. Kaisersberger, H.J. Flammersheim, Thermochim. Acta 391 (2002) 119.
[27] H.J. Flammersheim, J.R. Opfermann, Thermochim. Acta 337 (1999) 141.
[28] H. Bockhorn, A. Hornung, U. Hornung, D. Schawaller, J. Anal. Appl. Pyrol. 48 (1999) 93.
[29] T. Faravelli, G. Bozzano, M. Colombo, E. Ranzi, M. Dente, J. Anal. Appl. Pyrol. 70 (2003) 761.
[30] B. Saha, A.K. Maity, A.K. Ghoshal, Thermochim. Acta 444 (2006) 46.
[31] B. Saha, A.K. Ghoshal, Thermochim. Acta 451 (2006) 27.
[32] B. Saha, A.K. Ghoshal, Ind. Eng. Chem. Res. 45 (2006) 7752, doi:10.1021/ie060282x.
[33] J.G.A.P. Filho, E.C. Graciliano, A.O.S. Silva, M.J.B. Souza, A.S. Araujo, Catal. Today 107/108 (2005) 507.
[34] S. Vyazovkin, V. Goriyachko, Thermochim. Acta 194 (1992) 221.
[35] S. Vyazovkin, C.A. Wight, Thermochim. Acta 340/341 (1999) 53.
[36] S. Vyazovkin, Thermochim. Acta 355 (2000) 155.
[37] S. Vyazovkin, C.A. Wight, Chem. Mater. 11 (1999) 3386.
[38] S. Vyazovkin, D. Dollimore, J. Chem. Inf. Comput. Sci. 36 (1996) 42.
[39] S. Vyazovkin, Int. J. Chem. Kinet. 28 (1996) 95.
[40] S. Vyazovkin, N. Sbirrazzuoli, Macromol. Rapid Commun. 27 (2006) 1515.
[41] J.D. Peterson, S. Vyazovkin, C.A. Wight, Macromol. Chem. Phys. 202 (2001) 775.
[42] R.E. Lyon, Thermochim. Acta 297 (1997) 117.